Critical analysis of magnetically semi-disordered systems: critical exponents at various transitions

1998 J. Phys.: Condens. Matter 10 1599

(http://iopscience.iop.org/0953-8984/10/7/010)

J. Phys.: Condens. Matter **10** (1998) 1599–1619. Printed in the UK PII: S0953-8984(98)85745-7

Critical analysis of magnetically semi-disordered systems: critical exponents at various transitions

A Belayachi†‡, J L Dormann† and M Noguès†

† Laboratoire de Magnétisme et d'Optique, CNRS–Université de Versailles, Bâtiment Fermat, 45 Avenue des Etats Unis, 78035 Versailles Cédex, France

‡ Laboratoire de Physique des Matériaux, Faculté des Sciences, Université Mohammed V, BP 1014 Rabat, Morocco

Received 30 June 1997, in final form 13 October 1997

Abstract. The critical analysis of various magnetically semi-disordered compounds with spinel structure is reported. The magnetic equation of state is valid in the vicinity of the different observed transitions and the critical exponents are determined by different methods. At the magnetic–paramagnetic transition, the critical exponents β and δ are larger and smaller respectively than those found for 3D Heisenberg ferromagnets. The exponent variations are explained phenomenologically and allow a classification of the compounds to be made according to the degree of disorder. At low temperature, for some materials a mixed state occurs below the re-entrant transition, characterized by critical exponents, while for other materials local canted states exist, where the transverse spin components block progressively, revealing an absence of a true phase transition. At high temperature, a well established spin-cluster regime occurs in some cases. Two transitions with critical exponents are evident, the magnetic–cluster and the cluster–paramagnetic transitions.

1. Introduction

Derived from general theory on phase transitions based on the concept that this transition is describable by an order parameter [1], the magnetic equation of state near the transition temperature T_C at which the transition to the paramagnetic phase occurs leads to a unique relationship between the normalized quantities $m = M_S/|t|^\beta$ and $h = H_{int}/|t|^{\beta\delta}$ with $t = 1 - T/T_C$, where M_S is the spontaneous magnetization, H_{int} is the internal field equal to the applied field corrected for the demagnetizing field and β and δ are the critical exponents. This equation can be written as follows:

$$m = f\left(h, \frac{t}{|t|}\right) = f_{\pm}(h) \tag{1}$$

which means that m is described as a function of h by two curves, $f_-(h)$ and $f_+(h)$ for $T < T_C$ and $T > T_C$, respectively.

For an ideal ferromagnet, the temperature dependence of the order parameter M_S and its derivative susceptibility $\chi = \partial M_S/\partial H_{int}$, which corresponds to the initial susceptibility, can be described by the following power laws:

$$M_S \propto t^\beta \qquad \text{for } T > T_C \text{ and } H_{int} = 0 \tag{2}$$

$$\chi' \propto (T_C - T)^{\gamma'} \qquad \text{for } T < T_C \text{ and } H_{int} = 0 \tag{3}$$

$$\chi \propto (T - T_C)^{\gamma} \qquad \text{for } T > T_C \text{ and } H_{int} = 0 \tag{4}$$

$$M_S \propto H_{int}^{1/\delta} \qquad \text{at } T = T_C. \tag{5}$$

0953-8984/98/071599+21$19.50

In fact, it can be demonstrated that only two of these critical exponents are independent and the others are related to them via the scaling law [2]

$$\gamma = \gamma' = \beta(\delta - 1). \tag{6}$$

The scaling analysis was applied firstly to Ni, CrO_2 and $CrBr_3$ [3–5] and later to numerous ferromagnet and ferrimagnet systems.

However, the γ-value for a three-dimensional ferromagnet ($\gamma \cong 1.38$) does not recover the Curie–Weiss behaviour

$$\chi = \frac{C_p}{T - \theta_p}$$

in the paramagnetic state. For this state, $\gamma = 1$ if $\theta_p = T_C$ or if $T \to \infty$. This fact has led to the introduction of an effective exponent $\gamma(T)$ defined by the following equation [6]:

$$\gamma(T) = (T_C - T)\frac{\partial(\ln \chi)}{\partial T} \tag{7}$$

which shows a monotonic variation from $\gamma \cong 1.38$ (near T_C) to $\gamma = 1$ ($T \to \infty$). We note that using the variable $t' = 1 - T_C/T$, which implies some slight modifications of the scaling hypothesis, allows one to reproduce the true paramagnetic properties with an exponent γ^+ now defined [7] as

$$\chi \propto \frac{(t')^{\gamma^+}}{T}. \tag{8}$$

However, we shall use the variable t in our analysis in order to compare our results to others, t being almost always used.

For a long time, much attention has been paid to studying the influence of quenched spatial order on the magnetic properties of amorphous ferromagnets [8]. The critical phenomena of such materials have received increasing experimental and theoretical attention [9–11]. In the case of these materials, it has been shown that the critical temperature range can be described by the homogeneous three-dimensional Heisenberg model. In contrast, whereas the temperature dependence of $\gamma(T)$ in the intermediate range is monotonic for homogeneous ferromagnets and ferrimagnets, there is a characteristic non-monotonic variation of $\gamma(T)$ for structurally disordered ferromagnets which has been explained by taking into account the fluctuation of the exchange integrals due to topological disorder [12].

Numerous studies have been devoted to the scaling analysis of magnetically semi-disordered or disordered systems for several reasons. Firstly, scaling properties reveal in principle a magnetic phase transition. In contrast, the absence of such properties indicates instead a progressive change of the magnetic state, such as the blocking process of the magnetic moments of fine particles [13]. Secondly, the values of the critical exponents allow features such as the kind of magnetic phase present, its dimensionality and the kind of disorder. Finally, the analysis permits the determination of the transition temperature, often difficult to measure by using other techniques. Three types of magnetic phase have been mainly investigated: the spin glasses, the re-entrant ferromagnets and systems with random anisotropy.

For spin glasses, for which M_S vanishes, the scaling laws are expected to be operant for non-linear magnetization because, for $T > T_g$, the magnetization is proportional to $1/|t|$ where $t = 1 - T/T_g$, which induces singular properties at T_g. Assuming a phase transition, the non-linear susceptibility χ_{nl} can be written [14] as follows:

$$\frac{\chi_{nl}}{|t|^\beta} = f\left(\frac{h^2}{|t|^{\beta+\gamma}}\right) \tag{9}$$

where $h = \mu_B g H/kT$.

However, the critical exponents which are found strongly differ from one system to another, probably due to the differences between the ranges of fields and temperatures for which the critical exponents were determined [15].

Another kind of system has attracted considerable interest during recent years, namely the re-entrant ferromagnets. From the theoretical point of view, different approaches have been taken in an effort to understand the occurrence of the re-entrant transition. On the basis of the mean-field theory for an Ising system, Sherrington and Kirkpatrick (SK) [16] reported the possibility of a transition from the ferromagnetic to the spin-glass phase, at low temperature, in random systems with mixed ferromagnetic and antiferromagnetic interactions. Gabay and Toulouse [17] extended the SK theory to a Heisenberg system and suggested the existence of two transition temperatures; they found that, at low temperature, an unsaturated long-range ferromagnetic order can coexist with a spin-glass phase among the transverse components of spins. Numerous experimental results (see for example references [18–22]) are to some extent in agreement with the theoretical predictions. General methods employing the scaling analysis for obtaining a simple form of the magnetic equation of state have been used for the ferromagnetic–paramagnetic transition and the re-entrant transition [23–28]. At the ferromagnetic–paramagnetic (FM–PM) transition, the exponents are generally close to the classical 3D Heisenberg values. A scaling of the magnetic isotherms was also obtained at the re-entrant transition temperature T_r. In this case, $t = T/T_r - 1$, which means that the branch f_- (magnetic in the FM–PM transition) corresponds to $T > T_r$, and hence to the (perturbed) ferromagnetic phase, and that the branch f_+ (paramagnetic in the FM–PM transition) corresponds to $T < T_r$, and hence to the mixed phase. The critical exponents determined depend sensitively on the systems studied; however, the δ-values are generally smaller than those found for the corresponding FM–PM transition while the β-values are similar.

Several studies [29–34] have reported critical phenomena in magnetic systems with either a weak or a strong random anisotropy, for which the spin direction varies from site to site. As predicted by Chudnovsky *et al* [35], four kinds of magnetic phase are observed when increasing the applied field. Firstly, a speromagnetic or sperimagnetic ordering takes place. The phase so created is very analogous to spin glasses in which the spins are frozen along their local anisotropy directions. Secondly, a correlated-spin-glass (CSG) state occurs, for which the spin directions are locally correlated but the total magnetization is zero. Thirdly, a ferromagnetic state with wandering axes (FWA) arises. Here, the resulting magnetization is not equal to zero and small deviations from the ferromagnetic order occur. Finally, at high field, an almost purely ferromagnetic phase exists. The field limit separating the different phases increases with the ratio D/J_0, where D is the anisotropy constant and J_0 the exchange integral. For speromagnetic order, the non-linear magnetization follows a spin-glass scaling [32–34], while for the FWA state, the ferromagnetic scaling is operant over wide ranges of h and t. The values of the critical exponents are generally not too far from those valid for 3D Heisenberg ferromagnets. However, for some systems [30], important deviations occur. The nature of the phase transition and the effects of a random anisotropy on the ferromagnetic critical behaviours, as a function of D/J_0, have been reported in reference [31].

In a preliminary work [36], we have shown that the ferromagnetic scaling is also operant in magnetically semi-disordered ferrites showing local canted states. The critical exponents β and δ were found to be respectively higher and lower than those found for a pure ferromagnet. In this work, we extend our study to various magnetically semi-disordered systems: ferrites, manganites, thio-chromite and seleno-chromite spinels, which present

local canted states, or re-entrant transition or spin-glass-like states, according to the system and the composition.

Table 1. Compositions of the samples studied.

System	Composition studied
A; $Cd_{1-x}Zn_xCr_2S_4$	$x = 0, 0.1, 0.2, 0.3, 0.4, 0.5$
B; $Cd_{1-x}Zn_xCr_2Se$	$x = 0.35, 0.45, 0.55$
C; $Li_{0.5+x/2}Ti_xFe_{2.5-3x/2}O_4$	$x = 1.20, 1.25, 1.32$
D; $Li_{0.5}Fe_{2.5-x}Al_xO_4$	$x = 1.75, 1.625, 1.5, 1.375$
E; $Zn_{1-x}Mg_xFe_2O_4$	$x = 0.1, 0.2, 0.3$
F; $Ni_xCd_{1-x}Mn_2O_4$	$x = 0.8, 0.6$

2. Experimental procedure

The samples studied are listed in table 1 together with their compositions. They correspond to various systems.

Systems A and B present spinel structure. The magnetic atom Cr^{3+} occupies the octahedral B sites. The frustrations arise from the coexistence of superexchange magnetic interactions of opposite signs: ferromagnetic J_1 between first neighbours and antiferromagnetic J_2 between first higher-order neighbours. The ratio J_1/J_2 depends on the type of ion (Zn or Cd) occupying the tetrahedral A sites and is sensitive to the fluctuations of the concentration; hence semi-disordered or disordered structures can be expected.

Systems C, D and E correspond to ferrite compounds. The magnetic atoms Fe^{3+} occupy both the tetrahedral sites A and the octahedral sites B, the Fe populations depending on the system and the composition. The magnetic atom concentrations at the two sites are roughly the same for systems C and D, while for system E the magnetic atoms are mainly at B sites.

System F also shows a spinel structure. It contains two magnetic atoms, Ni^{2+} mostly at B sites and anisotropic Mn^{3+} at both sites. For this system, the magnetic atom concentration is rather large, but a complex magnetic structure can be expected due to the effect of the strong anisotropy of Mn^{3+}. The preparation of all of the systems has been described elsewhere: for systems A and B in [37] and for systems C, D, E and F in [38], [39], [40] and [41], respectively.

Isothermal magnetization measurements for intermediate fields $0.01 \leqslant H \leqslant 1.8$ T have been performed for the temperature range 4.2–550 K by means of a vibrating-sample magnetometer (VSM). The high-field curves ($H \leqslant 20$ T) have been measured for the temperature range 4.2–300 K at the Service National des Champs Intenses (SNCI) at Grenoble.

3. General properties of the systems studied

All of the samples studied show a semi-disordered or disordered magnetic structure.

For system A, starting from a ferromagnetic state ($x = 0$, $T_C = 85$ K), re-entrant properties are observed for $0.1 \leqslant x \leqslant 0.2$, characterized by a plateau of the alternative (real-component) (a.c.) susceptibility for $T < T_C$ and a drop of χ'_{ac} at low temperatures. Two maxima of χ''_{ac} (the imaginary component of the ac susceptibility) are observed. When $x \geqslant 0.2$, the properties are gradually modified, leading to more disordered magnetic states.

For $x = 0.3$ and 0.4, χ'_{ac} shows a broad hump, centred at around 60 K, up to around 110 K. But no χ''_{ac}-maximum is detected. χ_{dc} shows an almost constant value over the range 60–110 K and falls rapidly at 115 K with large and strongly field-dependent irreversibilities. These puzzling properties can be explained as follows. Spin clusters can be expected below 120 K and grow up to 80 K, then merge in the infinite magnetic matrix at a certain temperature which corresponds to the transition from magnetic long-range order towards a cluster state. We remark that the cluster–paramagnetic transition temperature ($T_{\mathrm{cl}} \sim 115$ K) is higher than the T_C-value of the ferromagnet $CdCr_2S_4$ (85 K). In a homogeneous state, such an increase is not possible. For $x = 0.5$, the properties are very similar to spin-glass properties but the non-linear susceptibility does not diverge. This means that a true spin-glass transition does not occur and that spin-glass-like properties are present [42, 43].

For system B, several concentration ranges can be distinguished. For $x \leqslant 0.41$, the samples behave ferromagnetically. For $0.45 \leqslant x \leqslant 0.49$, the samples behave ferromagnetically but present, at low temperature, a decrease of the susceptibility with the temperature and irreversible phenomena. Thus, re-entrant properties are to be expected. For $0.52 \leqslant x \leqslant 0.575$, a broad maximum arises at around $T = 24$ K and irreversibilities occur below 11 K. Finally, for $0.6 \leqslant x \leqslant 1$, the samples behave antiferromagnetically and no transition is detected at low temperatures [44].

The properties of the three systems C [45–47], D [39, 48] and E [40, 49, 50] for the compositions studied are similar. A non-linear continuous increase of the magnetization with the applied field is observed at all temperatures until $H = 20$ T. This means that canted spin structure occurs for any temperature lower than T_N. However, in-field Mössbauer spectroscopy reveals a canted structure at low temperature but an apparent collinear structure above a certain temperature well below T_N. This has been interpreted in terms of local canted states, where the transverse spin component relaxes following a thermally activated process [45]. The zero-field-cooled and field-cooled magnetization measurements show strong irreversibilities as for a spin-glass-like state. These irreversibilities are strongly field dependent over the whole temperature range below T_N and disappear at intermediate fields. The irreversible phenomena depend on the coercive-field strength which is small just below T_N, but very high at very low temperature where a hysteresis loop time dependence is observed. Studies of the thermoremanence for system C show that the magnetic viscosity depends on the applied field and that, when increasing the temperature, the logarithmic slope first increases and then decreases. All of the low-field properties can be explained on the basis of a local canted structure, where the transverse spin component relaxes at high temperature and progressively blocks when decreasing the temperature. A review of the magnetic properties of substituted ferrites can be found in reference [51].

In the case of system F, the general properties described above for canted ferrites seem valid. However, at low temperature, it is certain that the anisotropy induced by Mn^{3+} ions modifies the properties, acting on the domain structure and on the canting angles. For a low substitution rate and at low temperature, the random substitution of diamagnetic ions at A sites causes a substantial canting at B sites, while for isotropic ferrite systems no canting is observed. This effect of random anisotropy leads to modification of the magnetic properties and results in local canted-state features. For high substitution rates, the properties are similar to those found for the spin-glass-like state [52].

4. Results

Examples of the temperature and applied field dependences of the magnetization are shown in figure 1 (SNCI measurements) and figure 2 (VSM measurements).

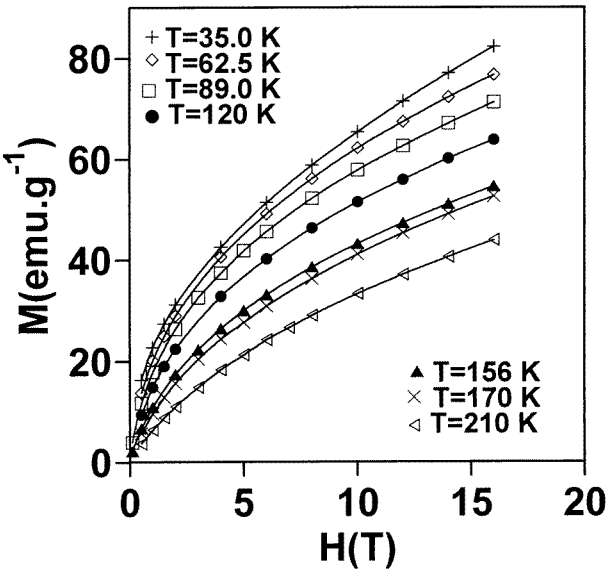

Figure 1. The temperature and field dependence of the magnetization for $Mg_{0.2}Zn_{0.8}Fe_2O_4$.

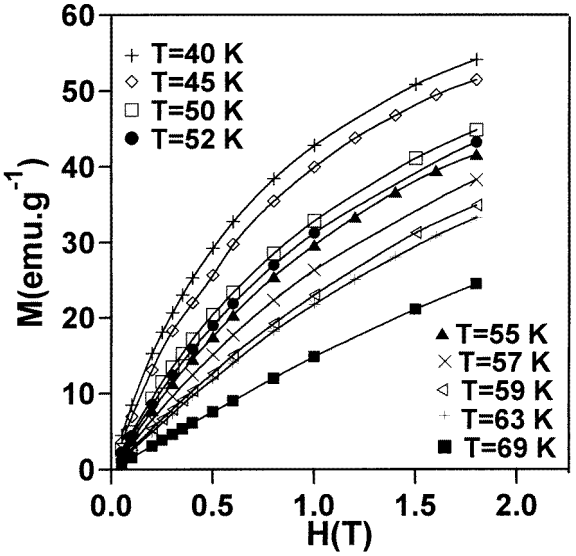

Figure 2. The temperature and field dependence of the magnetization for $Cd_{0.8}Zn_{0.2}Cr_2S_4$.

4.1. Methods for the determination of the critical exponents

For determining the critical exponents, we have used three methods: scaling plots, modified Arrott plots and δ-determination from the critical isotherm.

The scaling plots are based on equation (1), $m = f_{\pm}(h)$, where the plus and minus signs denote the ferromagnetic and paramagnetic regions respectively. Plotting $\ln(m)$ versus $\ln(h)$ yields data collapsing onto two branches if the parameters β, δ and T_C are correctly chosen.

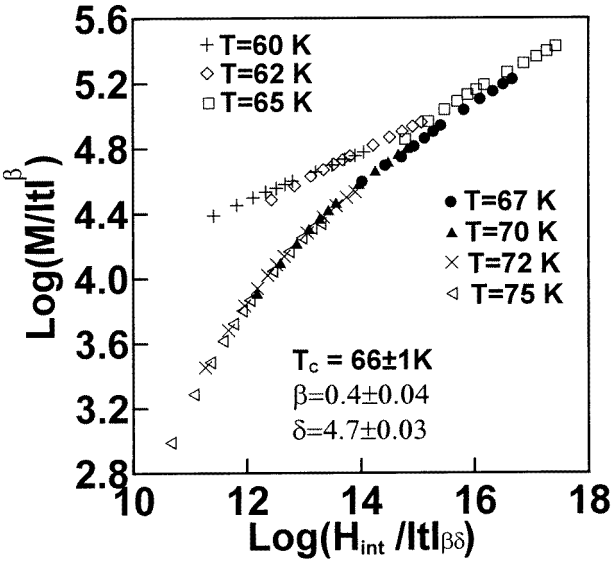

Figure 3. A scaling plot for $Cd_{0.65}Zn_{0.35}Cr_2Se_4$ at the magnetic transition.

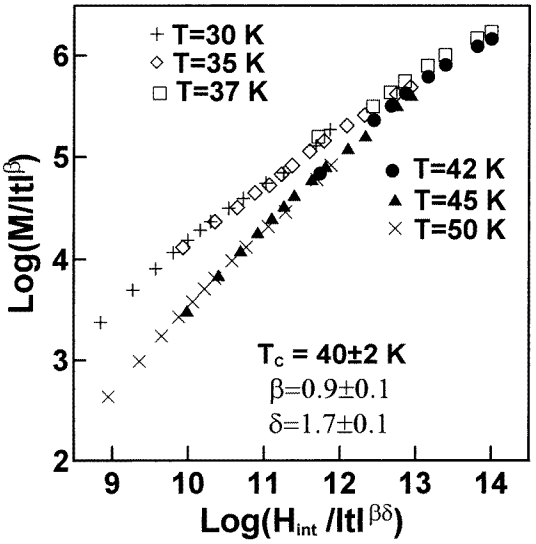

Figure 4. A scaling plot for $Cd_{0.7}Zn_{0.3}Cr_2S_4$ at the magnetic transition.

The upper branch represents the data for $T < T_C$ and the lower branch those for $T > T_C$. Examples of plots are shown in figures 3 to 7. In addition, the critical exponent γ can be calculated from equation (5). A difficulty occurs as regards the choice of the ranges of t and h in which the scaling operates. In ferromagnetic materials, these ranges are narrow but the exponent values could depend on the ranges chosen [53]. Therefore, we have used the following procedure. In a first step, we have considered all of the m- and h-values which collapse onto the two branches, taking into account the measurement accuracy. In a second

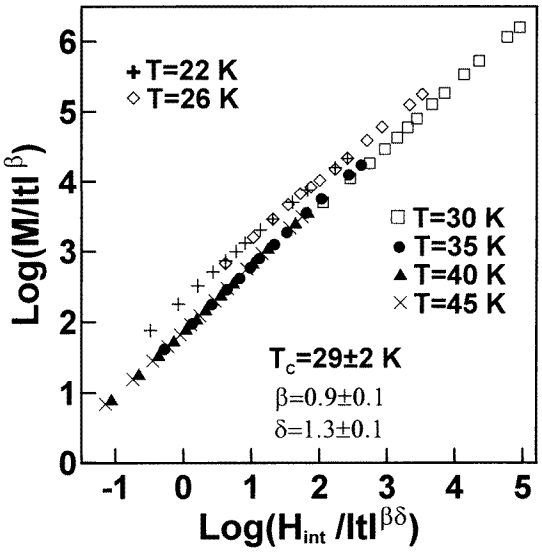

Figure 5. A scaling plot for $Cd_{0.6}Zn_{0.4}Cr_2S_4$ at the magnetic transition.

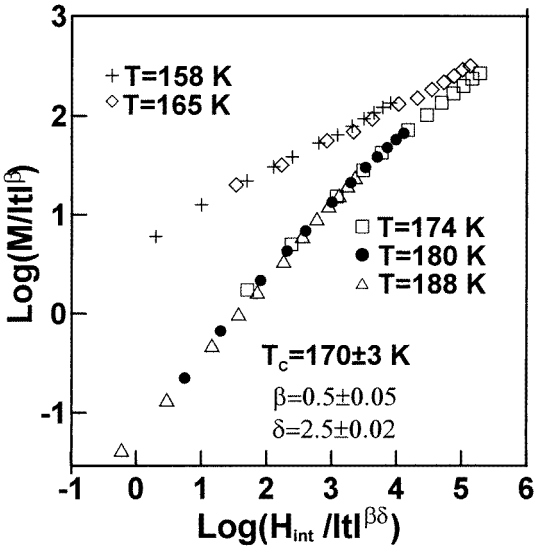

Figure 6. A scaling plot for $Li_{1.1}Ti_{1.2}Fe_{0.7}O_4$ at the magnetic transition.

step, we reduced as far as possible both the t- and h-ranges. No significant deviation for the critical exponents determined in the first step was observed for our samples. We note that we have used the internal field H_{int} for the scaling plots, i.e. the applied field corrected for the demagnetizing field evaluated from the sample shape.

The Arrott–Noakes equation [54], which was first postulated for the magnetic phase transition of pure nickel single crystal, is another independent possibility as a basis for the evaluation of the critical exponents β and γ from the measured isotherms. In the modified Arrott plot, the data are represented in the form $M^{1/\beta}$ versus $(H_{int}/M)^{1/\gamma}$ and the exponents

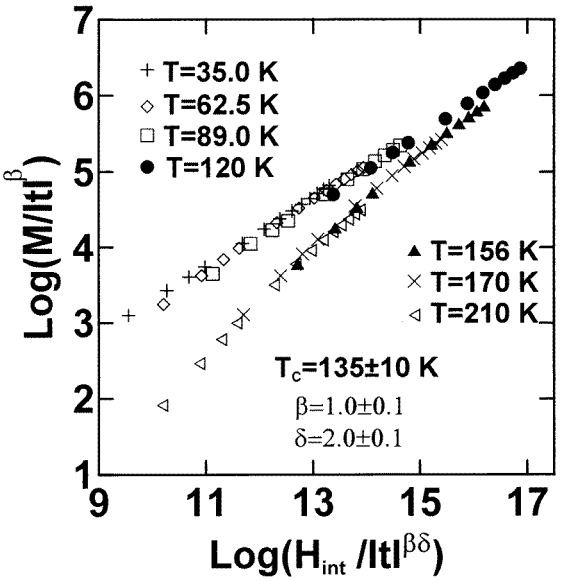

Figure 7. A scaling plot for $Mg_{0.2}Zn_{0.8}Fe_2O_4$ at the magnetic transition.

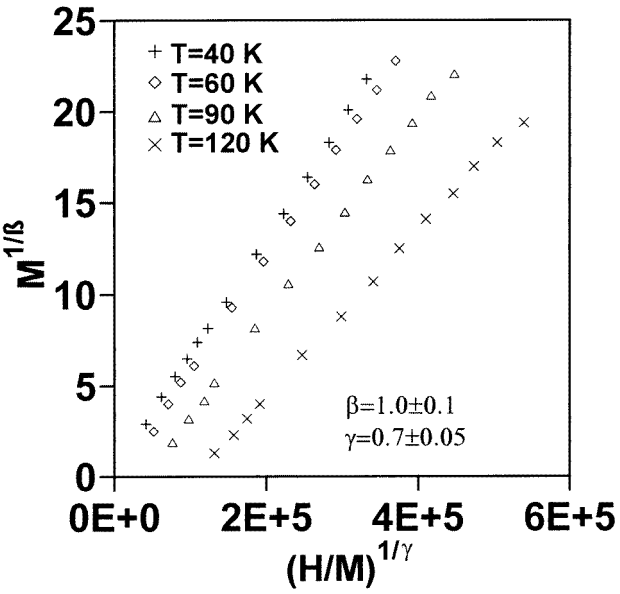

Figure 8. A modified Arrott plot for $Li_{0.5}Fe_{0.875}Al_{1.625}O_4$ at the magnetic transition.

β and γ are chosen in such a way that the isotherms around the critical one represent as closely as possible a set of straight lines, the critical isotherm ($T = T_C$) being the one which crosses the origin. A typical shape of graph is presented in figure 8. Equation (4) is assumed to be valid both below and above T_C, yielding the same susceptibility exponent $\gamma = \gamma'$ for both temperature regimes. We have tested the validity of the equation of state

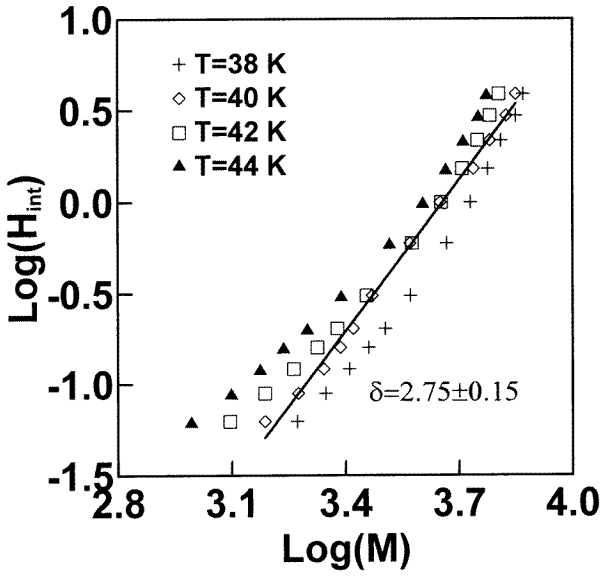

Figure 9. The field dependence of the critical isotherm for $Cd_{0.45}Zn_{0.55}Cr_2Se_4$ at the magnetic transition.

(4) by inserting, for the low-temperature isotherms $T < T_C$, a modified value of γ'. In all cases, the quality of the low-temperature plot deteriorates for $\gamma' \neq \gamma$, with a large scattering of the data around straight lines.

The field dependence of the magnetization on the critical isotherm $T = T_C$ is given by equation (5). Representing the data in the form $\ln(H_{int})$ versus $\ln(M)$ yields for $T = T_C$ a nearly straight line (figure 9) and the critical exponent δ can deduced from the slope.

4.2. Critical exponent values

For the magnetic–paramagnetic transition, critical exponents can be determined for all of the samples. The results are given in table 2. A good agreement is obtained between the three methods.

As we have discussed in the above section, some samples from systems A and B show at low temperature re-entrant transitions. On the other hand, for the ferrite systems C, D and E, the low-temperature properties resemble re-entrant properties. Hence, we have tried to apply the scaling laws near the re-entrant transition (systems A and B) and near the possible re-entrant transition for the other systems. In this case, the same equation of state is valid, with now $t = T/T_r - 1$. We have only succeeded for systems A and B, and the results are indicated in table 3. An example of a scaling plot is shown in figure 10. For the other systems, additional magnetization isotherms have been measured for the temperature region in which the transition could occur in order to ascertain that the scaling cannot operate.

Finally, for some samples, a cluster regime is well established over a certain temperature range below the transition temperature T_{cl} (see the section above). For these samples, the transition temperatures obtained from the scaling at the magnetic transition (table 4) are well below the temperature at which true paramagnetic properties first appear. Therefore, we have tried to apply the scaling to the cluster–paramagnetic transition. The results are given in table 4 and one example of a scaling plot is shown in figure 11.

Table 2. Critical temperatures and critical exponents for the magnetic–paramagnetic transition as derived from different methods: scaling plots (SP), modified Arrott plots (MAP) and critical isotherms (CI) for the samples studied. In the case of scaling plots, the exponent γ is calculated from equation (6). The ranges of t- and H-values for which the scaling plots are valid are also given (H in tesla).

	SP				MAP		CI	Validity range	
System; x	T_C	β	δ	γ	β	γ	δ	t	H
A; 0	84 ± 1	0.38	4.9	1.5	0.40	1.4	4.65	−0.06, 0.08	0.01, 1.8
A; 0.2	53 ± 2	0.9	1.9	0.8	0.9	1.0	4.95	−0.25, 0.3	0.01, 1.8
A; 0.3	40 ± 2	0.9	1.7	0.65	0.9	0.7	1.8	−0.25, 0.3	0.01, 1.8
A; 0.4	29 ± 2	0.9	1.3	0.3	1.2	0.25	1.7	−0.25, 0.55	0.01, 1.8
A; 0.5	19 ± 1	1.2	1.2	0.24	1.15	0.25	1.2	−0.16, 0.55	0.01, 1.8
B; 0.35	66 ± 1	0.4	4.7	1.5	0.40	1.45	4.85	−0.09, 0.13	0.01, 1.8
B; 0.45	52 ± 2	0.42	4.7	1.55	0.40	1.50	4.75	−0.15, 0.12	0.01, 1.8
B; 0.55	42 ± 2	0.5	2.8	0.9	0.50	0.9	2.75	−0.28, 0.19	0.01, 1.8
C; 1.20	170 ± 3	0.50	2.5	0.75	0.50	1.0	2.2	−0.07, 0.11	0.01, 1.8
C; 1.25	160 ± 5	0.9	2.0	0.8	1.0	1.0	2.1	−0.7, 0.4	0.1, 15
C; 1.32	70 ± 5	1.0	1.8	0.8	1.0	0.7	1.7	−0.8, 0.25	0.1, 20
D; 1.375	230 ± 20	0.7	2.2	0.85	0.7	0.85	$\leqslant 2.8$	−0.72, —	0.5, 20
D; 1.5	170 ± 10	0.9	1.9	0.8	0.90	0.80	1.9	−0.7, 0.3	0.5, 20
D; 1.625	75 ± 10	1.0	1.8	0.8	1.0	0.7	1.7	−0.5, 1.1	0.5, 20
D; 1.75	35 ± 5	1.2	1.35	0.42	1.2	0.40	1.35	−0.4, 1	0.5, 20
E; 0.3	200 ± 20	0.90	2.6	1.44	0.90	1.2	2.4	−0.8, 0.15	0.1, 20
E; 0.2	135 ± 10	1.0	2.0	1.0	1.0	0.90	1.9	−0.7, 0.55	0.1, 20
E; 0.1	75 ± 5	1.2	1.3	0.42	1.20	0.45	1.35	−0.7, 0.35	0.1, 20
F; 0.8	60 ± 3	0.7	1.8	0.56	0.70	0.60	1.7	−0.6, 0.3	0.5, 16
F; 0.6	35 ± 2	0.7	1.8	0.56	0.70	0.70	1.8	−0.6, 0.4	0.5, 16
Accuracy		10%	7%	10%	10%	10%	5%		

Table 3. Critical temperatures and critical exponents for the re-entrant transition as derived from different methods: scaling plots (SP) and critical isotherms (CI) for samples where the scaling is operant. For the scaling plots, the exponent γ_r is calculated from formula (6). The ranges of t and H for which the SP is valid are also given (H in tesla).

	SP				CI	Validity range	
System; x	T_r	β_r	δ_r	γ_r	δ_r	t	H
A; 0.2	18 ± 1	0.9	1.5	0.45	1.4	−0.1, 0.1	0.01, 0.4
A; 0.3	16 ± 1	0.9	1.45	0.41	1.45	−0.12, 0.12	0.01, 0.4
A; 0.4	13 ± 1	1.0	1.3	0.3	1.3	−0.15, 0.08	0.01, 0.4
B; 0.55	19 ± 1	0.5	1.5	0.25	1.5	−0.16, 0.16	0.02, 0.2
Accuracy		5%	5%	10%	5%		

5. Discussion

Our analysis of the critical behaviours has been carried out for spinel compounds which exhibit different types of magnetic order (ferromagnetism, perturbed ferromagnetism, mixed states and local canted states) and different types of transition (magnetic–paramagnetic, re-entrant and cluster–paramagnetic). We highlight three main results. Firstly, the different

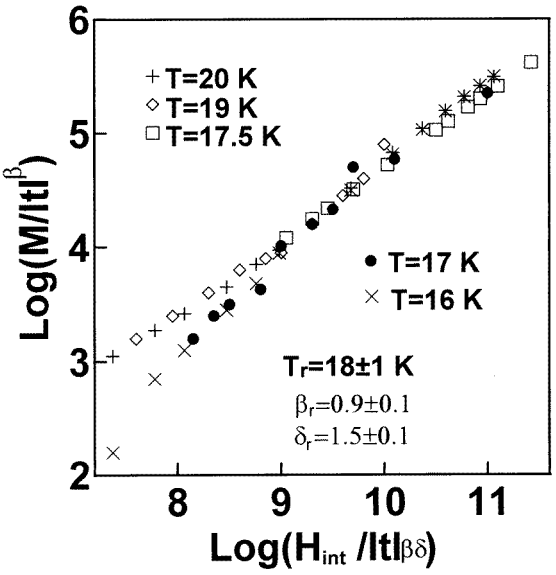

Figure 10. A scaling plot for $Cd_{0.8}Zn_{0.2}Cr_2S_4$ at the re-entrant transition.

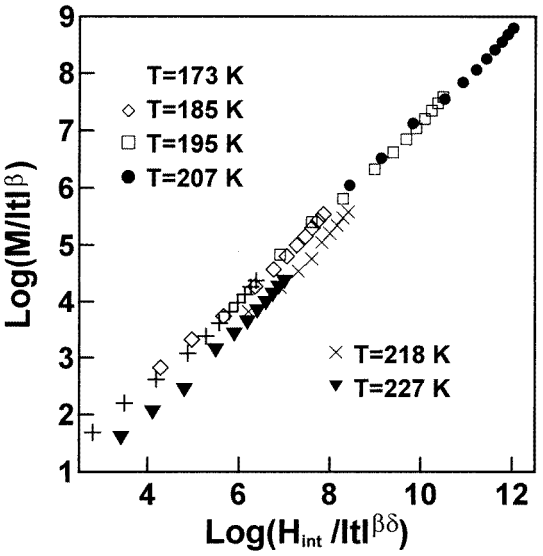

Figure 11. A scaling plot for $Li_{1.16}Ti_{1.32}Fe_{0.52}O_4$ at the cluster–paramagnetic transition.

methods which have been applied for the determination of the critical exponents lead to consistent results, within the error limits. Secondly, the scaling equation is found to be satisfied for all of the samples in the region of the magnetic transition. Finally, for some samples, the scaling is operant in the regions of the re-entrant transition and of the cluster–paramagnetic transition, revealing true phase transitions. We will discuss these results and the values of the critical exponents for (i) the magnetic transition, (ii) the re-entrant transition and (iii) the cluster–paramagnetic transition.

Table 4. Critical temperatures and critical exponents for the cluster–paramagnetic transition as derived from different methods: scaling plots (SP) and critical isotherms (CI) for the samples where the scaling is operant. For the scaling plot, the exponent γ_r is calculated from formula (6). The ranges of t and H for which the SP is valid are also given (H in tesla).

	SP				CI	Validity range	
System; x	T_{cl}	β_c	δ_c	γ_c	δ_c	t	H
A; 0.3	110 ± 5	2.3	1.2	0.46	1.2	−0.14, 0.31	0.01, 1.8
A; 0.4	110 ± 5	2.4	1.2	0.48	1.2	−0.18, 0.27	0.01, 1.8
A; 0.5	90 ± 5	2.1	1.1	0.42	1.1	−0.1, 0.33	0.01, 1.8
C; 1.32	210 ± 5	2.5	1.2	0.5	1.2	−0.15, 0.07	0.05, 1.8
F; 0.2	195 ± 10	2.2	1.2	0.44	1.1	−0.15, 0.14	0.01, 1.8
Accuracy		5%	5%	10%	5%		

Table 5. Typical values of the critical exponents for (1) 3D Heisenberg ferromagnets and (2) amorphous ferromagnets showing the re-entrant transition at low temperature.

	Material	T_C	β	δ	γ	Reference
(1)	CrO_2, Ni	627	0.378	4.58	1.34	[3]
	Ni	386	0.34	5.79	1.63	[3, 4]
	CrB_3	33	0.368	4.30	1.215	[5]
	$Fe_{84}B_{16}$	588	0.38	4.30	1.38	[8]
(2)	$Fe_{10}Pd_{72}Si_{18}$	48	0.4	5.0	1.60	[58]
	$Gd_{72}Ga_{18}B_{10}$	111	0.48	4.8	1.82	[27]
	$(Fe_{0.68}Mn_{0.32})_{75}P_{16}B_6Al_3$	100	0.4	5.3	1.72	[25]

Table 6. Typical values of the critical exponents for materials with random anisotropy in the FWA state (see the text); also given is the ratio of the anisotropy constant D to the exchange integral value J_0 and the applied field range for which the scaling is valid (H in tesla).

Material	D/J_0	T_C	β	δ	γ	H	Reference
$Tb_{65}Co_{35}$	0.32	89.1	0.46	4.5	1.61	0.1, 5.5	[29]
$(Dy_{0.914}Y_{0.086})Al_2$	0.66	47.5	1	2.5	1.5	—	[30]
$(Dy_{0.625}Y_{0.375})Al_2$	—	27.5	0.61	2.9	1.16	0.03, 0.5	[30]
$Nd_{50}Co_{50}$	0.008	164	0.39	4.0	1.17	0.01, 5.5	[31]

5.1. Magnetic transitions

Firstly, let us recall some typical values of the critical exponents for 3D Heisenberg ferromagnets, amorphous compounds showing a re-entrant transition at low temperature (table 5) and materials with a random anisotropy (table 6). We remark that, for amorphous compounds and for some of the materials with a random anisotropy, the exponent values are not too far from those found for Heisenberg ferromagnets ($\beta = 0.3639$, $\delta = 4.743$ and $\gamma = 1.3873$ [55]) with a β-value slightly higher, while for the other compounds with a random anisotropy, strong deviations are observed.

For our samples, the exponent values found for three compounds, i.e. $CdCr_2S_4$ (system A), and $Cd_{0.65}Zn_{0.35}Cr_2Se_4$ and $Cd_{0.55}Zn_{0.45}Cr_2Se_4$ (system B), are similar to the values

expected for Heisenberg ferromagnets. For the first compounds, the exponents are equal within the error limits to the theoretical values [55], while for the others a slight increase of β and a slight decrease of γ are observed, like for amorphous compounds showing re-entrant transitions. This is in agreement with the magnetic properties, which reveal a ferromagnetic order where the perturbations are not important. We note that the $Cd_{0.55}Zn_{0.45}Cr_2Se_4$ sample shows a re-entrant transition, which is not the case for the $Cd_{0.65}Zn_{0.35}Cr_2Se_4$ sample. However, this transition could be present at temperatures below the lowest measured temperature (8 K).

For the other samples, fairly strong deviations from Heisenberg ferromagnet values are observed for the critical exponents.

For system A, the disorders increase with x (see section 3). For $x = 0.2$, a re-entrant transition is observed. For $x = 0.3$ and 0.4, the properties are progressively modified, indicating a more disordered state. For example, the two peaks of the imaginary part of the alternative susceptibility, related to the paramagnetic–magnetic and re-entrant transitions, partially recover. For $x = 0.5$, spin-glass-like properties occur. The critical exponents show an increase of β and a decrease of δ with increasing x, i.e. with increasing magnetic disorder.

For $Cd_{0.45}Zn_{0.55}Cr_2Se_4$ (system B), a re-entrant transition is present and the magnetic properties indicate clearly a more disordered magnetic structure than for the other compositions of the system. We find $\beta = 0.5$ and $\delta = 2.8$, i.e. a slight increase of β and a net decrease of δ with respect to the Heisenberg ferromagnet values.

For systems B and C, the number of non-magnetic atoms increases with x, and the dilution of Fe^{3+} increases. These systems show local canted states (see section 3). With increasing Fe dilution, the distribution of the canting angles enlarges and the average canting angle increases at each site. As a consequence, the average magnitude of the transverse spin component S_t increases. Moreover, S_t becomes more and more widely distributed. Therefore, with increasing x, the magnetic disorder increases. For the exponent values, the same variations, i.e. an increase of β and a decrease of δ, are observed as for systems A and B, with increasing magnetic disorder.

For system E, the same variation is also observed. With decreasing x, the number of non-magnetic atoms at A sites increases. For the compositions studied, this number is large. At B sites, the number of non-magnetic atoms decreases, but in all cases, it is too small to perturb the magnetic order at A sites. Therefore, when decreasing x, the average canting angle at B sites increases and, like for systems C and D, the magnetic disorder increases.

In the case of system F, the magnetic disorder results from both the random substitution of non-magnetic atoms (Cd) at A sites and the anisotropic character of Mn^{3+}. We recall that for the pure compound ($NiMn_2O_4$), a complex triangular spin structure appears [52] and that the number of substituted non-magnetic atoms ($x = 0.2$ and 0.4) is not sufficient to destabilize the ferrimagnetic order in the case of isotropic magnetic ions [51]. For $x = 0.8$ and 0.6, the properties are similar to those observed for the samples belonging to systems C, D and E; however, it is difficult to evaluate the degree of magnetic disorder due to the interplay of the two causes. In fact, the same values for the critical exponents are found for the two compounds, with a strongly increased β-value and a strongly decreased δ-value with respect to the Heisenberg ferromagnet values.

In conclusion, we can say that when increasing the magnetic disorder, the exponent β increases and the exponent δ decreases.

In table 7, we have ranged the samples studied versus the decreasing δ-values. Homogeneous categories can be defined according to δ- and β-values as well as according to the magnetic properties.

Table 7. The critical exponent values found in order of decreasing δ. The γ-exponent is calculated from equation (6).

	δ	β	γ	Samples	
1	4.9	0.38	1.48	A; 0	Ferromagnetic or
	4.7	0.4	1.48	B; 0.35	very weak disorder
	4.7	0.42	1.55	B; 0.45	
2	2.8	0.5	0.9	B; 0.55	Appreciable disorder
	2.6	0.9	1.44	E; 0.3	
	2.5	0.5	0.75	C; 1.20	
3	2.2	0.7	0.84	D; 1.375	Intermediate disorder
	2.0	0.9	0.9	C; 1.25	
	2.0	1.0	1.0	E; 0.2	
	1.9	0.9	0.8	A; 0.2, D; 1.5	
	1.8	0.7	0.56	F; 0.8, F; 0.6	
	1.8	1	0.8	C; 1.32, D; 1.625	
	1.7	0.9	0.63	A; 0.3	
4	1.35	1.2	0.42	D; 1.75	Strong disorder
	1.3	0.9	0.27	A; 0.4	
	1.3	1.2	0.36	E; 0.1	
	1.2	1.2	0.24	A; 0.5	

The first category corresponds to exponent values very close to the 3D Heisenberg ferromagnet ones. Ferromagnetic phases are observed or very weak magnetic disorder. According to the typical values for various samples given in tables 5 and 6, not only does the 3D Heisenberg ferromagnet belong (of course) to this category, but also so do the amorphous ferromagnets showing re-entrant properties and two compounds with random anisotropy.

For the second category, magnetic properties reveal appreciable magnetic disorder. The δ-values range between 2.5 and 2.8 and the β-values are not too far from the ferromagnet value, except for the E(0.3) sample for which the classification remains ambiguous. The two other compounds with random anisotropy, cited in table 6, also belong to this category.

The third category corresponds to medium to strong magnetic disorder from a magnetic property point of view. δ ranges between 1.7 and 2.2 and β lies in the range 0.9–1.0, except for the sample D(1.375), which is intermediate between the second and third categories, and for the samples F ($\beta = 0.7$) whose magnetic disorder derives from two sources (random anisotropy and dilution of magnetic atoms). In this latter case, some deviations with respect to the other systems can be understood.

Finally, the fourth category corresponds to samples with strong to very strong magnetic disorder: spin-glass-like properties are found for the sample A(0.5), with the lowest δ-value. δ ranges between 1.2 and 1.35 and β between 0.9 and 1.2. γ-values will be discussed in section 5.3.

In our opinion, the shifts that we obtain for the δ- and β-values with respect to the 3D Heisenberg ferromagnet values are related to the degree of disorder. Therefore, the determination of the critical exponents can provide information on the degree of magnetic disorder.

It is interesting to note the variation of the relative position of the branches f_+ and f_- as a function of the exponent values (and the magnetic disorder). When they are close to the

Heisenberg ferromagnet values, the usual shape is obtained (figure 3), but when β increases and δ decreases, the branches approach progressively. For the second category (table 7; figure 6) the branches have nearly the usual shape. For the third category, the branches begin to approach (figures 4 and 7) and, finally, for the fourth category, the branches are close to one another (figure 5). In fact, when increasing the disorder, the differences between magnetic and paramagnetic phases (especially if a cluster regime occurs—see below) become less distinct. For example, in the paramagnetic regime, the spin moment relaxes very quickly. Below the transition temperature, the spin moment is static for true ferromagnets, while for local canted states the transverse spin component also relaxes very quickly. In addition, a distribution of transition temperatures probably occurs, smoothing the transition. In this case, the differences between the magnetic equations of state in magnetic (f_+) and paramagnetic (f_-) regimes reduce and the branches approach.

To understand the variations of β and δ with the magnetic disorder, let us recall two experimental properties. Firstly, the increase of the magnetization when decreasing the temperature from T_C is more and more smooth when the magnetic disorder increases. In fact, the magnetic order is well established only at low temperature due to the competing exchange interactions and frustrations, which induce the disorders. Secondly, the magnetic disorders consist in deviations from the averaged ferromagnetic or ferrimagnetic order. An applied field reduces the disorder and causes an appreciable increase of the magnetization, which is not the case for true ferromagnets. For example, for ferrite systems (C, D and E), the saturation is not observed until $H = 20$ T (figure 1). In this case, we can understand the variations observed for the critical exponents β and δ. Let us recall the power laws (2) and (5):

$$M_S \propto t^{\beta} \qquad \text{for } t > 0, t \to 0 \text{ and } H = 0 \tag{2}$$

and

$$M \propto H^{1/\delta} \qquad \text{at } t = 0. \tag{5}$$

On increasing β, the M_S-variation with t will be less, and on decreasing γ, the M_S-variation with H will be more pronounced. Of course, the power laws are strictly valid under the cited conditions (equations (2) and (5)), but the trends deduced also obtain for the other t- and H-values. In addition, due to the progressive increase of the magnetization with H and t, the ranges of H- and t-values for which the scaling is operant is extended with respect to those for true ferromagnetic materials.

Finally, let us note two features. Firstly, the scaling is always operant if the transition temperature is slightly distributed, in principle without modification of the critical exponents, which is not the case when the distribution is large. In our samples, particularly when clusters occur (see below), such a distribution could arise, which evidently smooths the variation of the magnetization with the temperature. Secondly, it is often difficult to determine the transition temperature from magnetic measurements, due to the smoothed variation of the magnetization (or the susceptibility). This is not the case according to scaling plots, from which an accurate value is obtained which corresponds to the averaged value of the transition temperature if a slight distribution of this temperature is present.

5.2. Re-entrant transitions

Compounds with competing interactions and frustration can show a mixed state below a certain temperature T_r in which the longitudinal spin component remains ferromagnetically or ferrimagnetically ordered and the transverse spin component S_t presents a spin-glass

state. Above T_r and below the magnetic–paramagnetic transition, the order is ferromagnetic or ferrimagnetic (see the introduction). In fact, some magnetic perturbations persist in this temperature range. Some properties reveal the mixed state, like a maximum in the imaginary part of the alternative susceptibility χ_{ac}, a drop of the real part (χ'_{ac}) and a strong increase of the coercive field at low temperature, as has been found for several compounds.

Table 8. Typical values of the critical exponents at the re-entrant transition for amorphous ferromagnets.

System	T_r (K)	β_r	δ_r	γ_r	Reference
$Fe_{10}Pd_{72}Si_{18}$	18	0.4	3.5	1.0	[58]
$Gd_{72}Ga_{18}B_{10}$	40	0.4	4.0	1.2	[27]
$(Fe_{0.68}Mn_{0.32})_{75}P_{16}B_6Al_3$	38	0.4	4.5	1.4	[25]

At the re-entrant transition, the scaling is operant, with now $t = T/T_r - 1$ (see the introduction) which leads to the inversion of the branches of the magnetic equation of state with respect to the magnetic–paramagnetic transition (f_- corresponding now to the low-temperature range). Typical values of the critical exponents β_r, δ_r and γ_r at the re-entrant transition are given in table 8 for the same compounds as in the lower part of table 5. One can see that δ_r is smaller than δ and $\beta_r = \beta$, δ and β being the exponents at the magnetic–paramagnetic transition.

For our samples, the magnetic properties reveal a re-entrant transition for some compounds of systems A and B. For the other systems, the interpretation is more difficult. Some properties are in agreement with the expected properties at the re-entrant transition while other properties, such as the continuous increase of the magnetization for any temperature below the magnetic transition, are somewhat in contradiction with the existence of a re-entrant transition.

Therefore, we have tried to apply the scaling equation around the possible re-entrant transition for all of the compounds studied. For systems A and B, it is not difficult to determine the temperature region, while this is not the case for the other systems; the temperature of the drop of the zero-field-cooled magnetization (or χ'_{ac}) is only a first approach. Additional isotherm magnetization measurements have been performed for some samples in order to confirm the results. They show that scaling plots are operant only for some samples of systems A and B (table 3) and that they are not operant for 8 K $< T < T_N$ for the other systems.

This latter result confirms our interpretation derived for local canted states [51]. For these states, the transverse spin component S_t exists below the transition temperature and relaxes very quickly between energy minima following a thermally activated process. Hence, for low-field measurements (or Mössbauer spectroscopy), the magnetic state appears collinear, when, for high-field measurements, canted structures are revealed. When decreasing the temperature from T_N, S_t blocks progressively and at low temperature local canted states are similar to mixed states. In this case, the scaling cannot operate because the blocking process is progressive versus temperature and the blocking temperatures are distributed. These features rule out the interpretation of the properties of similar systems in terms of re-entrant transitions.

For system A, scaling is operant for $x = 0.2$, 0.3 and 0.4, but not for $x = 0.5$. This is in agreement with the magnetic measurements. For $x = 0.5$, a spin-glass-like state occurs and therefore only one transition is expected. For system B, the properties are less clear from magnetic measurement data. For $x = 0.45$, a re-entrant transition could be expected,

while for $x = 0.55$, it is difficult to choose between two transitions (including the re-entrant transition) and only one (spin-glass-type order). The scaling is operant only for $x = 0.55$, ruling out the possibility of the occurrence of this latter state. However, for $x = 0.45$, for which the scaling is not operant, a re-entrant transition could occur at a temperature smaller than our lowest measurement temperature (8 K), which could explain why we have not been able to scale the magnetization. Finally, β_r is close to β and δ_r is slightly smaller than δ, like for amorphous compounds.

5.3. Cluster–paramagnetic transitions

True paramagnetic properties are not found in the vicinity of the magnetic–paramagnetic transition (see the introduction). In the critical temperature region, for $t < 0$, the susceptibility is described by the power law (3), i.e. $\chi \sim (-t)^{-\gamma}$, with $\gamma = 1.38$ for 3D Heisenberg ferromagnets. This law recovers Curie–Weiss behaviour, i.e. $\chi = C_p/(T - \theta_p)$, only if $\gamma = 1$ and $T \to \infty$ (except that the latter condition is not necessary in the very special case where $T_C = \theta_p$).

In the case of a well established Curie–Weiss regime, outside the critical regime, the Kouvel–Fisher exponent (equation (7)) is equal to

$$\gamma(T) = \frac{T - T_C}{T - \theta_p}. \tag{7a}$$

Therefore, $\gamma(T)$ shows a monotonic variation and tends to 1 when $T \to \infty$, with $\gamma(T) < 1$ for $\theta_p < T_C$.

However, in insulating systems where competing interactions occur, which causes frustration and magnetic disorder, the Curie–Weiss regime is often well established only for temperatures substantially higher than the critical temperature range. This could be due to the existence, in the intermediate-temperature range, of a short-range spin order. In this type of system, this order could consist in very small spin clusters of different sizes, which behave superparamagnetically. In this case, the susceptibility is described by a Curie–Weiss-type law where the Curie-like parameters (the constant C and the temperature θ) are related to the magnetic moments of the clusters [13]. When increasing the temperature, the clusters evolve, and they disappear when the paramagnetic regime is reached. Thus, we observe for $\gamma(T)$ firstly a constant value in the critical regime and secondly a variation in the intermediate regime following (7*a*). In this case, non-monotonic variation of $\gamma(T)$ is possible, as observed for some compounds, such as $Zn_xNi_{1-x}Fe_2O_4$ [56].

Nevertheless, in some cases, the Curie-like C-parameter remains constant over a certain range of temperature above the critical regime. This means that the spin clusters do not evolve in this temperature range. As an example, the variation of the inverse of the susceptibility for $Li_{1.16}Ti_{1.32}Fe_{0.52}O_4$ [57] is shown in figure 12. In the so-called paramagnetic phase, two regimes are clearly evident. In this case, we can expect that firstly the scaling is operant at T_C, since just above the critical regime there is no important difference between a spin-cluster regime which evolves and one which is stabilized, and that secondly the scaling is perhaps operant at the temperature at which the stabilized cluster regime evolves toward a true paramagnetic phase.

At the magnetic transition, the γ-exponents decrease when the magnetic disorder increases (table 7). As in section 5.1, a rough classification can be obtained by considering decreasing γ-values instead of decreasing δ-values, though the classification according to δ-values seems to be in better agreement with the magnetic properties. On the other hand, the compounds showing a cluster–paramagnetic transition (table 4) belong to the bottom of

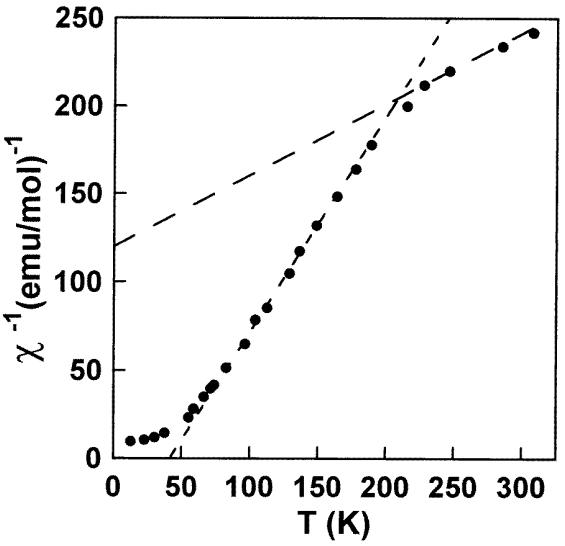

Figure 12. The temperature dependence of the inverse susceptibility above the magnetic transition for $Li_{1.16}Ti_{1.32}Fe_{0.52}O_4$.

category 3 and to category 4 (table 7). Thus, these compounds correspond to more disordered systems, but do not show particular δ- and β-values with respect to the compounds of the same category for which no cluster–paramagnetic transition has been found. This shows that in the critical region, γ does not depend very much on the type of the cluster regime, as we discussed above.

Spin clusters can be characterized by weak interactions between clusters, smaller than the thermal energy, and strong interactions inside the clusters. These conditions can be fulfilled only if the number of lacking magnetic bonds, randomly distributed, is important. This is realized in our compounds if the number of non-magnetic atoms is high (systems C, D or E). However, it depends on the system, because either the distribution of the magnetic atoms at the two sites and (or) the exchange integral values are not the same, or the ferromagnetic and antiferromagnetic interactions almost cancel (systems A or B).

From magnetic properties, a well characterized cluster regime is found for the A(0.3), A(0.4), C(1.32) and F(0.8) samples, but for the other samples, such as A(0.5), it is impossible to reach a conclusion. However, if the scaling is operant at the cluster–paramagnetic transition for the samples with a well characterized cluster regime, then it is also for the A(0.5) sample. The exponent values are very similar for the samples, with $2.2 \leqslant \beta_c \leqslant 2.5$, $\delta_c \approx 1.2$ and $\gamma_c \approx 0.47$. We remark that, for this transition, the $f_\pm$ are almost linear functions. This leads to $\chi \approx$ constant $\times\ |t|^{-\beta_c(\delta_c-1)} \approx$ constant $\times\ |t|^{-\gamma_c}$. In this case, the uncertainties in β_c and δ_c are large and only γ_c can be relied upon. On the other hand, the true paramagnetic regime is not reached in the critical region of the cluster–paramagnetic transition, as γ_r is different from one, but this can be due to the difference between the cluster–paramagnetic transition temperature $T_{\rm cl}$ and θ_p.

6. Conclusions

In conclusion, we have shown that the magnetic equation of state is valid in the vicinity of the magnetic–paramagnetic transition for various spinel compounds showing magnetic phases that are semi-disordered to greater and lesser extents. With increasing magnetic disorder, the critical exponents β and δ deviate from 3D Heisenberg ferromagnet values,

the former increasing and the latter decreasing. The exponent variations are explained phenomenologically and allow a classification of the compounds according to the degree of disorder. Moreover, the scaling plots permit a precise knowledge of the transition temperature to be established, which is often difficult purely from magnetic measurements. In some materials, the scaling is operant at the re-entrant transition at low temperature, but we show that it is not operant when the magnetic order consists in local canted states arising in diluted two-magnetic-sublattice systems. This definitively establishes the difference between mixed and local canted states where for the former a phase transition occurs for the transverse spin component S_t at the re-entrant transition while for the latter only a progressive blocking of S_t occurs. For some compounds which present a well established spin-cluster regime above the magnetic transition, we show that the scaling is operant as expected at this transition, but also at the cluster–paramagnetic transition where the clusters disappear. This demonstrates that the latter transition is a true phase transition, of which the critical exponents are derived for the first time. Finally, we want to underline that the study of scaling properties allows us to deduce numerous features, such as the existence of phase transitions, the nature of the magnetic phases and the precise values of the transition temperatures.

References

[1] Kadanoff L P, Götze W, Hamblen D, Hecht R, Lewis E A S, Pelciauskas V V, Rayl M, Swift J, Aspnes D and Kane J 1967 *Rev. Mod. Phys.* **39** 395
[2] Stanley H E 1971 *Introduction to Phase Transitions and Critical Phenomena* (Oxford: Clarendon)
[3] Kouvel J S and Rodbell D S 1967 *Phys. Rev. Lett.* **18** 215
[4] Kouvel J S and Comly B 1968 *Phys. Rev. Lett.* **20** 1237
[5] Ho J T and Litster J D 1969 *Phys. Rev. Lett.* **22** 603
[6] Kouvel J S and Fisher M E 1969 *Phys. Rev.* **136** 1626
[7] Carré E and Souletie J 1988 *J. Magn. Magn. Mater.* **72** 29
[8] Kakehashi Y 1991 *Phys. Rev.* B **43** 10 820
Kakehashi Y 1993 *Phys. Rev.* B **47** 3185
[9] Kaul S N 1985 *J. Magn. Magn. Mater.* **53** 5
[10] Reisser R, Seeger M and Kronmüller H 1993 *J. Magn. Magn. Mater.* **128** 321
[11] Nicolaides G K, Hadjipanayis G C and Rao K V 1993 *Phys. Rev.* B **48** 12 759
[12] Fähnle M 1983 *J. Phys. C: Solid State Phys.* **16** L819
Fähnle M 1987 *J. Magn. Magn. Mater.* **65** 1
[13] Dormann J L, Fiorani D and Tronc E 1997 *Adv. Chem. Phys.* **98** 283
[14] Omari R, Prejean J J and Souletie J 1983 *J. Physique* **44** 1069
[15] Bouchiat H 1986 *J. Physique* **47** 71
[16] Sherrington D and Kirkpatrick K 1975 *Phys. Rev. Lett.* **35** 1792
[17] Gabay M and Toulouse G 1981 *Phys. Rev. Lett.* **47** 201
[18] Manns V, Brand R A and Keune W 1983 *Solid State Commun.* **48** 811
[19] Brand R A, Lauer J and Keune W 1985 *Phys. Rev.* B **31** 1630
[20] Mazumdar P and Bhagat S M 1987 *J. Magn. Magn. Mater.* **66** 263
[21] Kouvel J S, Abdul-Razzaq W and Ziq Kh 1987 *Phys. Rev.* B **35** 1768
[22] Hesse J, Böttger Ch, Wulfes A, Sievert J and Ahlers H 1993 *Phys. Status Solidi* a **135** 343
[23] Salamon M B, Rao K V and Chen H S 1980 *Phys. Rev. Lett.* **44** 596
[24] Yeshurun Y, Salamon M B, Rao K V and Chen H S 1980 *Phys. Rev. Lett.* **45** 1366
[25] Salamon M B, Rao K V and Yeshurun Y 1981 *J. Appl. Phys.* **52** 1687
[26] Geohegan J A and Bhagat S M 1981 *J. Magn. Magn. Mater.* **25** 17
Manheimer M A, Bhagat S M and Chen H S 1983 *J. Magn. Magn. Mater.* **38** 147
[27] O'Shea M J and Sellmyer D J 1985 *Phys. Rev.* B **32** 7502
[28] Sellmyer D J, Muench G and O'Shea M J 1987 *J. Magn. Magn. Mater.* **65** 93
[29] Lee K M and O'Shea M J 1990 *J. Appl. Phys.* **67** 5781
[30] Gehring P M, Salamon M B, del Moral A and Arnaudas J I 1990 *Phys. Rev.* B **41** 9134

del Moral A, Arnaudas J I, Gehring P M, Salamon M B, Ritter C, Joven E and Cullen J 1993 *Phys. Rev.* B **47** 7892
[31] Lee K M and O'Shea M J 1993 *Phys. Rev.* B **48** 13 614
[32] Dieny B and Barbara B 1986 *Phys. Rev. Lett.* **57** 1169
[33] Sellmyer D J and Nafis S 1986 *Phys. Rev. Lett.* **57** 1173
[34] Lee K M, O'Shea M J and Sellmyer D J 1987 *J. Appl. Phys.* **61** 3616
[35] Chudnovsky E M, Saslow W M and Serota R A 1986 *Phys. Rev.* B **33** 251
[36] Dormann J L, Belayachi A and Noguès M 1992 *J. Magn. Magn. Mater.* **104–107** 239
[37] Agostinelli E, Battistoni C, Fiorani D, Mattogno G and Noguès M 1989 *J. Phys. Chem. Solids* **50** 269
[38] Noguès M, Dormann J L, Perrin M, Simonnet W and Gibart P 1979 *IEEE Trans. Magn.* **15** 1729
[39] Noguès M, Dormann J L, Maknani J, Villers G and Dumond Y 1989 *Advanced in Ferrites* ed C M Srivastava and M J Patni (New Delhi: Oxford and IBH) p 347
[40] Zemirli M, Grenèche J M, Varret F, Lenglet M and Teillet J 1988 *J. Physique* **49** 917
[41] Bhandage G T and Keer H V 1987 *J. Mater. Sci. Lett.* **6** 109
[42] Noguès M, Fiorani D, Tejada J, Dormann J L, Sayouri S, Testa A M and Agostinelli E 1992 *J. Magn. Magn. Mater.* **104–107** 1641
[43] Agostinelli E, Aurisicchio C, Battistoni C, Dormann J L, Fiorani D, Mattogno G and Noguès M 1987 *Proc. 7th ICTMC* (Pittsburgh, PA: Materials Research Society) p 515
[44] Noguès M and Dormann J L 1986 *J. Magn. Magn. Mater.* **54–57** 87
[45] Dormann J L, El Harfaoui M, Noguès M and Jové J 1987 *J. Phys. C: Solid State Phys.* **20** L161
[46] Seqqat M, Dormann J L, Noguès M, Jové J and Renaudin P 1994 *Hyperfine Interact.* **94** 2017
[47] Godinho M, Carvalho A, Noguès M, Dormann J L and Seqqat M 1994 *J. Magn. Magn. Mater.* **133** 457
[48] Maknani J, Dormann J L, Noguès M, Varret F and Teillet J 1990 *Hyperfine Interact.* **54** 603
[49] Teillet J, Hauet A, Noguès M and Dormann J L 1991 *Hyperfine Interact.* **68** 345
[50] Noguès M, Dormann J L, Teillet J and Villers G 1992 *J. Magn. Magn. Mater.* **104–107** 415
[51] Dormann J L and Noguès M 1990 *J. Phys.: Condens. Matter.* **2** 1223
[52] Bhandage G T, Belayachi A, Noguès M, Villers G, Dormann J L and Keer H V 1997 *J. Magn. Magn. Mater.* **166** 141
[53] Fähnle M, Kellner W U and Kronmüller H 1987 *Phys. Rev.* B **35** 3640
[54] Arrott A and Noakes J E 1967 *Phys. Rev. Lett.* **19** 786
[55] Chen K, Ferrenberg A M and Landau D P 1993 *Phys. Rev.* B **48** 3299
[56] Haug M, Fähnle M, Kronmüller H and Haberey F 1987 *J. Magn. Magn. Mater.* **69** 163
Haug M, Fähnle M, Kronmüller H and Haberey F 1987 *Phys. Status Solidi* b **144** 411
[57] Seqqat M 1981 *Thèse* Université S Mohammed Ben Abdellah, Morocco
[58] Dublon G and Yeshurun Y 1982 *Phys. Rev.* B **25** 4899